Since January 2020 Elsevier has created a COVID-19 resource centre with free information in English and Mandarin on the novel coronavirus COVID-19. The COVID-19 resource centre is hosted on Elsevier Connect, the company's public news and information website.

Veterinary Microbiology 257 (2021) 109068

Contents lists available at ScienceDirect

Veterinary Microbiology

journal homepage: www.elsevier.com/locate/vetmic

Ergosterol peroxide suppresses porcine deltacoronavirus (PDCoV)-induced autophagy to inhibit virus replication *via* p38 signaling pathway

Cong Duan [1], Yi Liu [1], Zhihui Hao, Jiufeng Wang *

College of Veterinary Medicine, China Agricultural University, Beijing, 100193, China

ARTICLE INFO

Keywords:
Porcine deltacoronavirus
Ergosterol peroxide
Autophagy
p38 signaling pathway

ABSTRACT

Porcine deltacoronavirus (PDCoV) is a swine enteropathogenic coronavirus (CoV) that continues to spread globally, placing strain on economic and public health. Currently, the pathogenic mechanism of PDCoV remains largely unclear, and effective strategies to prevent or treat PDCoV infection are still limited. In this study, the interaction between autophagy and PDCoV replication in LLC-PK1 cells was investigated. We demonstrated that PDCoV infection induced a complete autophagy process. Pharmacologically induced autophagy with rapamycin increased the expression of PDCoV N, while pharmacologically inhibited autophagy with wortmannin decreased the expression of PDCoV N, suggesting that PDCoV-induced autophagy facilitates virus replication. Further experiments showed that PDCoV infection activated p38 signaling pathway to trigger autophagy. Besides, ergosterol peroxide (EP) alleviated PDCoV-induced activation of p38 to suppress autophagy, thus exerting its antiviral effects. Finally, we employed a piglet model of PDCoV infection to demonstrate that EP prevented PDCoV infection by suppressing PDCoV-induced autophagy *via* p38 signaling pathway *in vivo*. Collectively, these findings accelerate the understanding of the pathogenesis of PDCoV infection and provide new insights for the development of EP as an effective therapeutic strategy for PDCoV.

1. Introduction

Porcine deltacoronavirus (PDCoV) is a swine enteropathogenic coronavirus (CoV), which belongs to the genus *Deltacoronavirus* of the family *Coronaviridae*. It can cause severe dehydration, vomiting and watery diarrhea in piglets (Ma et al., 2015), leading significant economic loss in the swine industry. PDCoV was first detected in 2012 in pig feces during the molecular surveillance of CoVs (Woo et al., 2012), and first broke out in the United States in February 2014 with 30–40 % mortality in piglets (Wang et al., 2014). Subsequently, it has been found in many countries, including South Korea, Japan and China (Dong et al., 2016; Jang et al., 2017; Suzuki et al., 2018). In addition to pigs, PDCoV can infect a variety of other animals, including calves and poultry (Boley et al., 2020; Jung et al., 2017), highlighting its potential to cross interspecies barriers. As an emerging virus, the pathogenesis and virus-host interaction of PDCoV are poorly understood. Besides, effective therapeutics or vaccines to control PDCoV infection are still limited.

Autophagy is an evolutionarily conserved process to maintain cellular homeostasis in response to stress (*e.g.* nutrient and energy deficiency, pathogen infection, and endoplasmic reticulum stress) *via* formation of a double-membraned autophagosome and subsequent lysosomal fusion leading to degradation (Boya et al., 2013). However, several viruses have evolved diverse strategies to hijack autophagy for their own benefit, such as classical swine fever virus (CSFV), porcine reproductive and respiratory syndrome virus (PRRSV) and porcine epidemic diarrhea virus (PEDV) (Lin et al., 2020; Pei et al., 2014; Sun et al., 2012). Understanding the relationship between autophagy and viral infection is crucial to control the disease (Bonam et al., 2020). PDCoV infection has been reported to induce autophagy (Qin et al., 2019), but no study has shown how PDCoV causes autophagy and the functions of autophagy during PDCoV replication the details. The p38 mitogen-activated protein kinase (MAPK) signaling pathway is a major cell signaling pathway which converts extracellular stimuli into a wide range of cellular responses, including autophagy (Gan et al., 2018; Hou et al., 2020). We previously demonstrated that PDCoV infection activated p38 signaling pathway to benefit its replication (Duan et al., 2021). Therefore, we are curious whether p38 signaling pathway is involved in autophagy induced by PDCoV infection.

* Corresponding author at: College of Veterinary Medicine, China Agricultural University, No. 2 Yuanmingyuan West Road, Beijing, 100193, China.
E-mail address: jiufeng_wang@hotmail.com (J. Wang).
[1] Cong Duan and Yi Liu are equal first authors.

https://doi.org/10.1016/j.vetmic.2021.109068
Received 17 February 2021; Accepted 6 April 2021
Available online 10 April 2021

Our recent study has shown that ergosterol peroxide (EP) from the mushroom *Cryptoporus volvatus* (*C. volvatus*) possesses efficient anti-PDCoV properties and can alleviate p38 activation induced by PDCoV infection (Duan et al., 2021). *C. volvatus* belongs to the family *Aphyllophorales* and the genus *Cryptoporus*, and grows in certain areas in China (Hua et al., 1991). It has a long medical use history for treating asthma and bronchitis in China. Aqueous extracts from the fruiting body of *C. volvatus* have been reported to have multiple bioactivities, such as anti-tumorigenic, anti-allergic, anti-inflammatory and antiviral activities (Ma et al., 2013; Xie et al., 2006; Zhu et al., 2016).

In the present study, we employed LLC-PK1 cell models and piglet models of PDCoV infection to reveal the relationship between autophagy and PDCoV infection, and to elucidate the mechanisms by which PDCoV infection induced autophagy. Moreover, we explored the inhibitory effects of EP on PDCoV infection from the viewpoint of autophagy.

2. Materials and methods

2.1. Ethics in animal experimentation

Experiments with piglets were carried out in strict accordance with the Guidelines for Laboratory Animal Use and Care from the Chinese Center for Disease Control and Prevention and the Rules for Medical Laboratory Animals from the Chinese Ministry of Health, under protocol CAU20190816-1, approved by the Animal Ethics Committee of China Agricultural University.

2.2. Preparation of EP

EP was extracted from *Cryptoporus volvatus* with a purity of over 97 %. Extraction and purity determination were done as previously described (Duan et al., 2021).

2.3. Cell culture

LLC-PK1 cells (ATCC CL-101) were obtained from the American Type Culture Collection (ATCC) and cultured in MEM (Gibco, USA) supplemented with 1% antibiotic-antimycotic (Gibco, USA), 1% HEPES (Gibco, USA), 1% MEM non-essential amino acids solution (NEAA) (Gibco, USA) and 10 % heat-inactivated fetal bovine serum (FBS) (Gibco, Australia). LLC-PK1 cells were incubated at 37 °C with 5% CO_2.

2.4. Virus, viral infection and virus titration

The PDCoV CHN-HN-1601 strain (GenBank accession no: MG832584) provided by Professor Hanchun Yang, China Agricultural University, was used in this study. Virus titers were calculated using the Reed-Muench method and expressed as 50 % tissue culture infectious doses per milliliter ($TCID_{50}$/mL). LLC-PK1 cells were grown to 80 % confluence in 6-well plates and incubated with PDCoV at a multiplicity of infection (MOI) of 2 with 10 μg/mL trypsin for 1 h at 37 °C. After being washed three times with phosphate-buffered saline (PBS), the cells were cultured in maintenance medium without FBS supplemented with 5 μg/mL trypsin. Suspended virus was irradiated with UV light for 5 h with gentle shaking at intervals to prepare inactivated PDCoV.

2.5. Indirect immunofluorescence assay (IFA)

LLC-PK1 cells were washed with PBS and fixed with 4% paraformaldehyde for 30 min at 4℃. The cells were permeabilized with 0.2 % Triton X-100 for 10 min. After washing with PBS, the cells were blocked with 1% bovine serum albumin (BSA) for 45 min at 37℃. Subsequently, the cells were stained with anti-PDCoV monoclonal antibody (1:1000, provided by Professor Pinghuang Liu, China Agricultural University, Beijing, China) at 4℃ for 12 h. The cells were then washed and incubated with FITC-conjugated goat anti-pig IgG (1:200, Solarbio, China) for 45 min at 37℃. After 3washes with PBS, the cells were examined by fluorescence microscopy (Olympus IX71, Tokyo, Japan).

2.6. Cytotoxicity assay

The cytotoxicity of rapamycin (Selleck, USA), wortmannin (Selleck, USA) and chloroquine (CQ, Sigma-Aldrich, Germany) were assessed *in vitro* using the Cell Counting Kit-8 (CCK-8, DOJINDO, Japan) according to the manufacturer's instructions. LLC-PK1 cells were seeded into 96-cell plates and grown to 100 % confluence for 24 h. After washing 3 times with PBS, the cells were treated with different concentrations of rapamycin, wortmannin and CQ. Mock-treated cells were used as control. After 36 h, the cells were washed with PBS and incubated with 100 μL MEM and 10 μL CCK-8 solution at 37℃ for 2 h. Absorbance was measured with a microplate reader (Model 680 Microplate Reader, BIO-RAD, USA) at 450 nm. Cytotoxicity was analyzed according to the following formula:

$$\text{Cytotoxicity (\%)} = [(\text{Abs sample}) - (\text{Abs blank})] / [(\text{Abs negative control}) - (\text{Abs blank})] \times 100$$

2.7. Intervention test of biochemical agents

Cells grown to 80 % confluence in 6-well plates were pretreated with autophagy activator rapamycin (62.5 μg/mL), autophagy inhibitor wortmannin (5 μg/mL), lysosomal inhibitor CQ (12.5 μg/mL) or p38 inhibitor SB203580 (5 μM) for 4 h, followed by PDCoV adsorption for 1 h at a MOI of 2. Then the inoculum was removed, and the cells were washed three times with PBS. Subsequently, the cells were cultured in fresh medium containing rapamycin (31.2 μg/mL), wortmannin (2.5 μg/mL), CQ (6.25 μg/mL) or p38 inhibitor SB203580 (5 μM). The cells were detected for the related indexes at 24 h post infection (hpi).

2.8. Confocal immunofluorescence microscopy

For the detection of autophagosomes, the cells were grown to 60–80 % confluence on glass coverslips in 6-well plates, then transfected with plasmid GFP-LC3 (provided by Wenqi He, Jilin University) using Lipofectamine 3000 (Invitrogen, USA) for 24 h. After three washes with PBS, the cells were infected with PDCoV (MOI = 2) for 1 h. Then the inoculum was removed, and the cells were washed three times with PBS. Subsequently, the cells were cultured in fresh medium. For the detection of autophagic flux, the cells were transfected with the tandem fluorescent monomeric red fluorescent protein (mRFP)-GFP-LC3 (ptfLC3) (provided by Wenqi He, Jilin University) as described above. After 24 h, the cells were washed and treated with CQ according to the method in the Intervention test of biochemical agents. At 24 hpi, the cells were washed with PBS and fixed with 4% paraformaldehyde for 30 min at 4℃. Cell monolayers were permeabilized with 0.2 % Triton X-100 for 10 min. The cells were then blocked with 1% BSA for 45 min at 37℃. Subsequently, the cells were stained with anti-PDCoV N monoclonal antibody (1:1000, Medgene, USA) at 4℃ for 12 h, followed by incubation of RBITC-conjugated goat anti-mouse IgG (1:200, Solarbio, China) for 45 min at 37℃. After washing with PBS, the cells were incubated with DAPI (Sigma-Aldrich, Germany) at room temperature for 5 min and photographed using a Leica SP8 Laser Scanning confocal microscope (Leica Microsystems, Germany).

2.9. Small interfering RNA (siRNA) transfection

Specific porcine p38 siRNA sequences were designed using the sequence of Sus scrofa p38 mRNA (GenBank Accession No. XM_003356616.1) and synthesized by Genepharma (Shanghai, China).

NC siRNA (5′-UUCUCCGAACGUGUCACGUTT-3′) was purchased from Genepharma. The p38 siRNA sequences were as follows: 5′- CCGAGGUCUCAAGUAUAUATT-3′ (#1), 5′-GGGCAGAUCUGAACAACAUTT-3′ (#2) and 5′-GCAGGAGCUGAACAAGACATT-3′ (#3). The siRNAs were transfected using HiPerFect Transfection Reagent (Giagen, Germany) at a final concentration of 60 nM according to the manufacturer's instructions. After 24 h, the efficiency of the siRNA was characterized by western blot.

2.10. Antiviral assays

The cells were infected with PDCoV (MOI = 2) in the absence or presence EP (150 μM). According to our previous study (Duan et al., 2021), treatment of LLC-PK1 cells with 150 μM EP for 36 h has no toxic effects. After 1 h, the inoculum was removed, and the cells were washed three times with PBS. Subsequently, the cells were cultured in fresh medium in the absence or presence EP (150 μM) for 1 h. The cells were collected and the related indexes were detected by western blot at 24 hpi.

2.11. In vivo study of piglets

A total of 15 seven-day-old crossbred (Landrace × Large White) piglets of mixed gender, weighing 3.0 ± 0.2 kg were purchased from a regular commercial farm in Tianjin, China. Prior to the start of the trial, no clinical signs of diarrhea or other diseases were observed in any of the piglets, and the rectal swabs were confirmed negative for the major porcine enteric viruses (PDCoV, porcine epidemic diarrhea virus (PEDV), transmissible gastroenteritis virus (TGEV) and rotavirus) by Reverse transcription PCR. On day 0, the piglets were divided randomly into 3 groups (n = 5 per group): (i) control group (CN), oral administration of 5 mL MEM at 8:00 am on days 1–3; (ii) PDCoV group, oral administration of 5 mL MEM containing a total of 1×10^6 $TCID_{50}$ of the PDCoV CHN-HN-1601 strain at 8:00 am on day 1, 5 mL MEM at 8:00 am on days 2-3; (iii) PDCoV + EP group, oral administration of 5 mL MEM containing a total of 1×10^6 $TCID_{50}$ of the PDCoV CHN-HN-1601 strain and EP (2.5 mg/kg body weight) at 8:00 am on day 1, 5 mL MEM containing EP (2.5 mg/kg body weight) on days 2-3. On day 5, piglets from each group were necropsied, and jejunal tissues were collected.

2.12. Western blot analysis

The cell and jejunum tissues were lysed in radioimmunoprecipitation assay (RIPA) lysis buffer (CoWin Biosciences, China) with 1 mM phenylmethyl sulfonyl fluoride (PMSF, Beyotime, China) and 20 μM NaF on ice. Primary antibodies used in this study were anti-LC3, anti-p62/SQSTM1 (1:1000, Sigma-Aldrich, Germany), anti-PDCoV N (1:5, provided by Professor Pinghuang Liu, China Agricultural University), anti-phospho-p38 (1:500, Cell Signaling Technology, USA), anti-p38 (1:1000, Cell Signaling Technology, USA) and anti-β-actin (1:1000, ProteinTech Group, USA). Horseradish peroxidase conjugated to AffiniPure goat anti-mouse IgG (1:5000, ProteinTech Group, USA) or goat anti-rabbit IgG (1:5000, ProteinTech Group, USA) was used as secondary antibodies.

2.13. Statistical analysis

All experiments were performed 3 times. Statistical analysis was performed using IBM SPSS Statistics 25 software (IBM, USA). Differences between means were compared using Tukey's honestly significant difference post-hoc test. The data were visualized using GraphPad Prism 7 software (GraphPad Software, USA) and expressed as mean ± SEM. The statistically significant differences were set at $P < 0.05$.

3. Results

3.1. PDCoV infection induces autophagy in LLC-PK1 cells

To explore whether PDCoV induces autophagy, the levels of autophagy marker proteins were examined in PDCoV-infected LLC-PK1 cells. LC3 is a specific marker protein for monitoring autophagic vesicle formation, and the ratio of LC3-II to β-actin is commonly used to assess the activity of autophagy. We found that LC3-II expression was significantly upregulated at 6, 12, 24 and 30 hpi, as compared with mock cells (Fig. 1A, B). PDCoV-induced autophagy was also determined by visualizing the fluorescent puncta of LC3. In agreement with western blot analysis, there was few fluorescent puncta in uninfected LLC-PK1 cells, whereas PDCoV-infected cells displayed accumulation of fluorescent puncta (Fig. 1D).

The accumulation of autophagosomes may be due to autophagy induction or a block in autophagosome maturation. To confirm whether PDCoV-induced autophagy is a complete process, we also measured the degradation of p62, a marker for the autophagy-mediated protein degradation pathway (Mizushima et al., 2010). PDCoV-infected cells decreased p62 expression at 6, 12, 24 and 30 hpi, as compared with mock cells (Fig. 1A, C), suggesting that PDCoV induced complete autophagy. To further confirm the observation, LLC-PK1 cells were transfected with a ptfLC3 plasmid. The signal of green (GFP) is quenched by the low pH inside the lysosome lumen, whereas the red signal (RFP) retains its fluorescence in acidic conditions. Meanwhile, LLC-PK1 cells were treated with CQ, which can inhibit the fusion of the autophagosome with lysosome. As shown in Fig. 1F, numerous red fluorescent puncta were observed and many green fluorescent puncta were quenched in PDCoV-infected cells at 24 hpi. In contrast, CQ treatment dramatically recovered green fluorescent puncta and increased yellow puncta in PDCoV-infected cells. These data indicated that PDCoV infection not only increased autophagosome formation, but also enhanced autophagic flux.

3.2. PDCoV replication enhances the autophagy process

To determine whether PDCoV induced-autophagy required virus replication, UV inactivation of PDCoV was performed. Loss of infectivity was confirmed by fluorescence imaging (Fig. 2A). LC3-II expression in cells infected with UV-inactivated PDCoV was higher than that in mock cells (Fig. 2B), however, lower than that in cells infected with the nonirradiated PDCoV (Fig. 2B), indicating that PDCoV replication enhances the autophagy process. These results were further confirmed by confocal immunofluorescent analysis. There were more fluorescent puncta in PDCoV-infected cells compared with UV-PDCoV-infected cells (Fig. 2C).

3.3. Autophagy promotes PDCoV replication

Next, we investigated the effect of autophagy on PDCoV replication. Western blot analysis demonstrated that rapamycin treatment significantly increased the levels of LC3-II and PDCoV N, whereas, wortmannin treatment decreased the levels of LC3-II and PDCoV N (Fig. 3A). In addition, rapamycin treatment up-regulated the infectious titers of PDCoV. Conversely, wortmannin treatment reduced the infectious titers of PDCoV (Fig. 3B). These findings reveal that autophagy promotes PDCoV replication. The treatment concentration of rapamycin and wortmannin had no toxic effects on the cells compared with the mock-treatment (Fig. 3C, D).

3.4. Inhibition of PDCoV-induced autophagy by EP contributes to its antiviral effect

We previously observed that EP inhibits PDCoV replication. Here we explored the possible antiviral mechanisms of EP. Compared with the

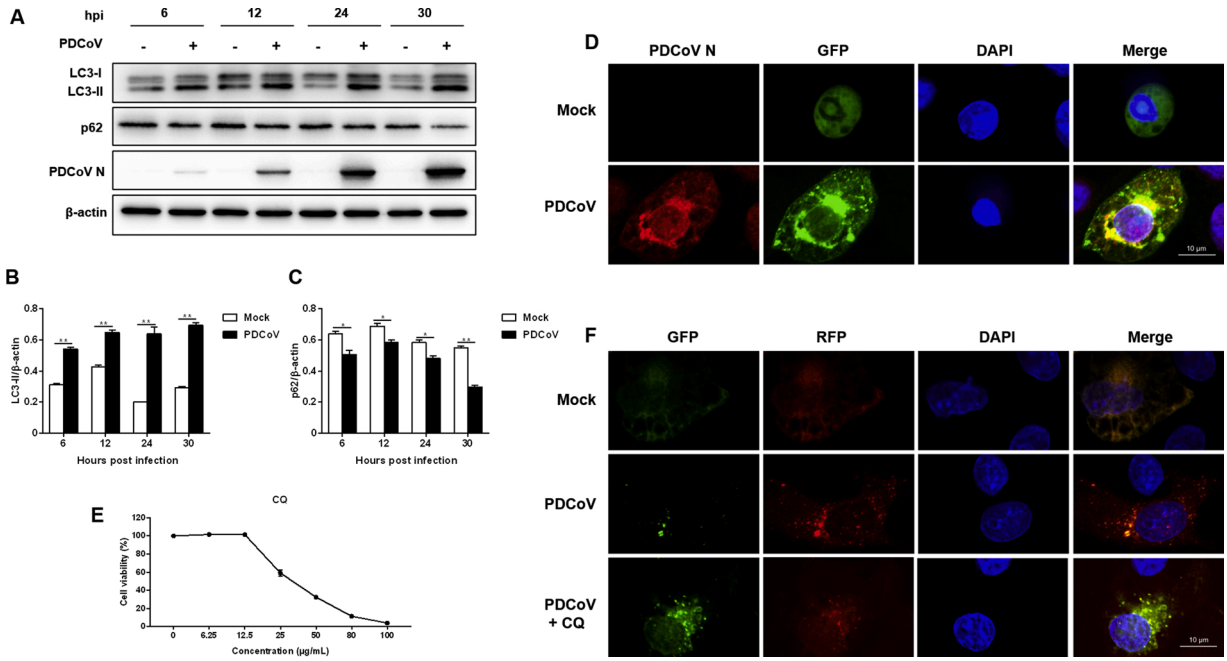

Fig. 1. PDCoV infection induces autophagy in LLC-PK1 cells. (A) LLC-PK1 cells were mock infected or infected with PDCoV (MOI = 2). The expressions of LC3-II and p62 were analyzed by western blot at 6, 12, 24 and 30 hpi. (B, C) Results were presented as the ratio of target protein band intensity to β-actin band intensity. (D) LLC-PK1 cells were transfected with plasmid GFP-LC3 for 24 h, followed by PDCoV infection (MOI = 2). The fluorescence signals were visualized by confocal immunofluorescence microscopy at 24 hpi. Scale bars: 10 μm. (E) Determination of cytotoxicity of CQ by CCK-8 assay. (F) LLC-PK1 cells were transfected with plasmid ptfLC3 for 24 h, followed by mock-treated or CQ (12.5 μg/mL)-treated for 4 h. Then, the cells were mock-infected or infected with PDCoV (MOI = 2). After PDCoV adsorption for 1 h, the cells were further cultured in fresh medium in the absence or presence of CQ (6.25 μg/mL). The fluorescence signals were visualized by confocal immunofluorescence microscopy at 24 hpi. Scale bars: 10 μm. Values represent the mean ± SEM for three independent experiments. $^{*}P < 0.05$; $^{**}P < 0.01$.

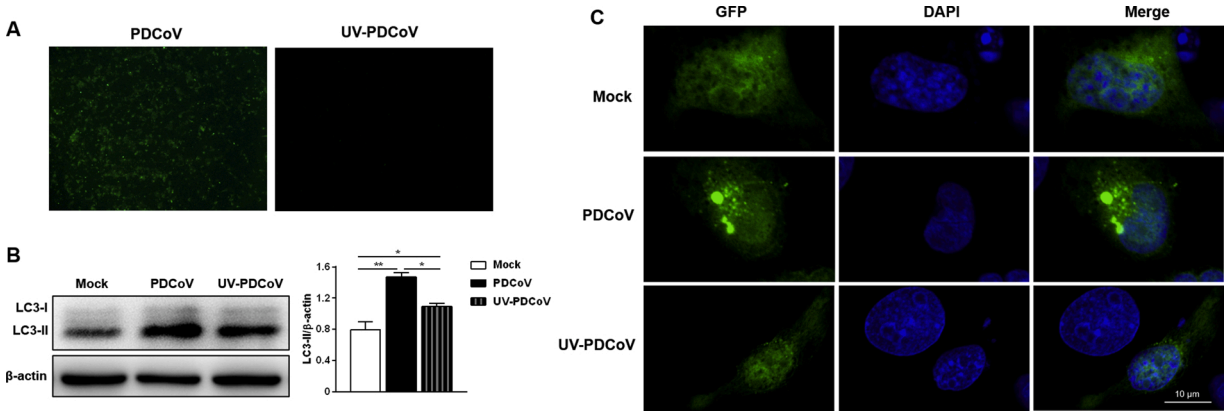

Fig. 2. PDCoV replication enhances the autophagy process. (A) Immunofluorescence assay verified that UV-inactivated PDCoV was replication defective. (B) LLC-PK1 cells were mock infected or infected with PDCoV and UV-inactivated PDCoV. The expression of LC3-II was analyzed by western blot at 24 hpi. Results were presented as the ratio of LC3-II band intensity to β-actin band intensity. (C) LLC-PK1 cells were transfected with plasmid GFP-LC3 for 24 h, followed by mock infected or infected with PDCoV and UV-inactivated PDCoV. The fluorescence signals were visualized by confocal immunofluorescence microscopy at 24 hpi. Scale bars: 10 μm. Values represent the mean ± SEM for three independent experiments. $^{*}P < 0.05$; $^{**}P < 0.01$.

cells infected with PDCoV only, EP treatment decreased the levels of LC3-II and PDCoV N (Fig. 4).

3.5. The p38 signaling pathway participates in the inhibition of EP on PDCoV-induced autophagy

Our previous study showed that PDCoV infection activated p38 signaling pathway to benefit its replication (Duan et al., 2021). The p38 signaling pathway has also been reported to mediate autophagy (Gan et al., 2018; Hou et al., 2020). Hence, we used p38 inhibitor SB203580, rapamycin and wortmannin to explore the role of p38 in PDCoV replication and PDCoV-induced autophagy. Infected cells treated with SB203580 had lower expressions of phosphorylated p38, LC3-II and PDCoV N compared with the cells infected with PDCoV only (Fig. 5A). Besides, SB203580 treatment reduced the infectious titers of PDCoV (Fig. 5B). A similar trend was observed in infected cells treated with wortmannin (Fig. 5A, B). However, increased expressions of phosphorylated p38, LC3-II and PDCoV N were observed in infected cells treated with rapamycin compared with the cells infected with PDCoV only (Fig. 5A). Consistently, rapamycin treatment increased the infectious titers of PDCoV (Fig. 5B). Next, we used siRNA-mediated knockdown to further address the role of p38 in EP inhibiting PDCoV replication and alleviating PDCoV-induced autophagy in LLC-PK1 cells. The siRNA targeting p38 apparently reduced the expression of p38 (Fig. 5C), and

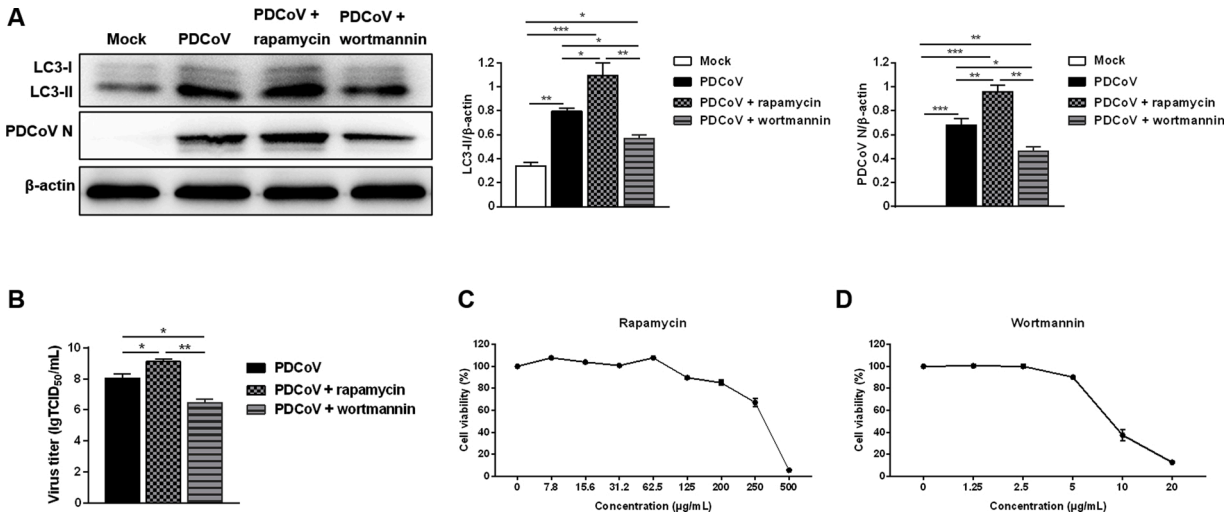

Fig. 3. Autophagy promotes PDCoV replication. (A) LLC-PK1 cells were pretreated with autophagy activator rapamycin (62.5 μg/mL) or autophagy inhibitor wortmannin (5 μg/mL) prior to PDCoV infection (MOI = 2). After PDCoV adsorption for 1 h, the cells were further cultured in fresh medium in the absence or presence of rapamycin (31.2 μg/mL) or wortmannin (2.5 μg/mL). The expressions of LC3-II and PDCoV N was analyzed by western blot at 24 hpi. Results were presented as the ratio of target protein band intensity to β-actin band intensity. (B) The virus titer ($lgTCID_{50}$/mL) in LLC-PK1 cell supernatants was calculated by the method of Reed and Muench. (C, D) Determination of cytotoxicity of rapamycin and wortmannin by CCK-8 assay. Values represent the mean ± SEM for three independent experiments. $^{*}P < 0.05$; $^{**}P < 0.01$; $^{***}P < 0.001$.

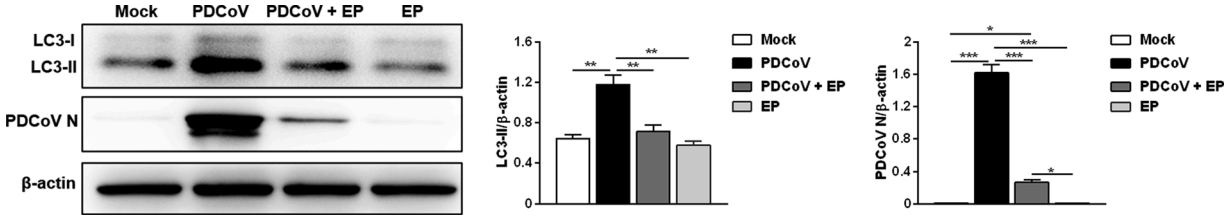

Fig. 4. Inhibition of PDCoV-induced autophagy by EP contributes to its antiviral effect. LLC-PK1 cells were mock-infected or infected with PDCoV (MOI = 2) in the absence or presence EP (150 μM). After PDCoV adsorption for 1 h, the cells were further cultured in fresh medium in the absence or presence EP (150 μM). The expressions of LC3-II and PDCoV N were analyzed by western blot at 24 hpi. Results were presented as the ratio of target protein band intensity to β-actin band intensity. Values represent the mean ± SEM for three independent experiments. $^{*}P < 0.05$; $^{**}P < 0.01$; $^{***}P < 0.001$.

p38 siRNA #1 was used for subsequent experiments. As shown in Fig. 5D, PDCoV infection increased the expression of phosphorylated p38 protein, and knockdown of p38 decreased the level of PDCoV N, implying that PDCoV might activate the p38 signaling pathway to facilitate its replication. Meanwhile, knockdown of p38 slowed down the increase of LC3-II expression induced by PDCoV infection, suggesting that p38 participates in the autophagy mechanism of PDCoV infection. EP treatment inhibited PDCoV-induced activation of p38, attenuated the up-regulated expression of LC3-II caused by PDCoV infection, and reduced the level of PDCoV N. Moreover, both knockdown of p38 and EP treatment decreased the infectious titers of PDCoV (Fig. 5E). These results demonstrated that EP could suppress PDCoV-induced autophagy to inhibit virus replication *via* p38 signaling pathway.

3.6. EP suppressed PDCoV-induced autophagy and p38 activation in the jejunum of piglets

Finally, we studied the autophagy induced by PDCoV and the effect of EP *in vivo*. As expected, all piglets in the PDCoV group showed typical clinical syndrome, including diarrhea and vomiting, while the piglets in the PDCoV + EP group and the CN group were normal. The jejunum villus structure of piglets in PDCoV group was incomplete, and the intestinal epithelial cells were shed. However, the jejunum of piglets in PDCoV + EP group only showed hyperaemia. Western blot analysis demonstrated that compared with the CN group, higher expression of LC3-II was observed in the jejunum of the PDCoV group (Fig. 6A, B). Conversely, lower expression of LC3-II was found in the jejunum of the PDCoV + EP group compared with the PDCoV group (Fig. 6A, B). There was no significant difference in LC3-II expression in the jejunum between the CN group and the PDCoV + EP group. These results indicated that administration of EP attenuated PDCoV-induced autophagy in piglets. In addition, the PDCoV group had higher expression of phosphorylated p38 in the jejunum compared with the CN group (Fig. 6A, C). However, expression of phosphorylated p38 in the jejunum of the PDCoV + EP group was lower than that of the PDCoV group (Fig. 6A, C). No statistical difference was found in phosphorylated p38 expression in the jejunum between the CN group and the PDCoV + EP group. These results suggested that administration of EP alleviated the activation of p38 induced by PDCoV in piglets. Correspondingly, it was observed that expression of PDCoV N in the jejunum of the PDCoV + EP group was obviously lower than that of the PDCoV group (Fig. 6A, E).

4. Discussion

Since 2014, PDCoV has disseminated around the world, causing significant economic losses to the pig industry. Until now, there is paucity of information on the underlying mechanism of PDCoV replication and pathogenesis. Autophagy has been widely investigated due to its important role in the pathogenesis of many diseases in recent years (Levine and Kroemer, 2008; Valero-Muñoz et al., 2020). It not only serves a protective function in cell survival under stress, but also

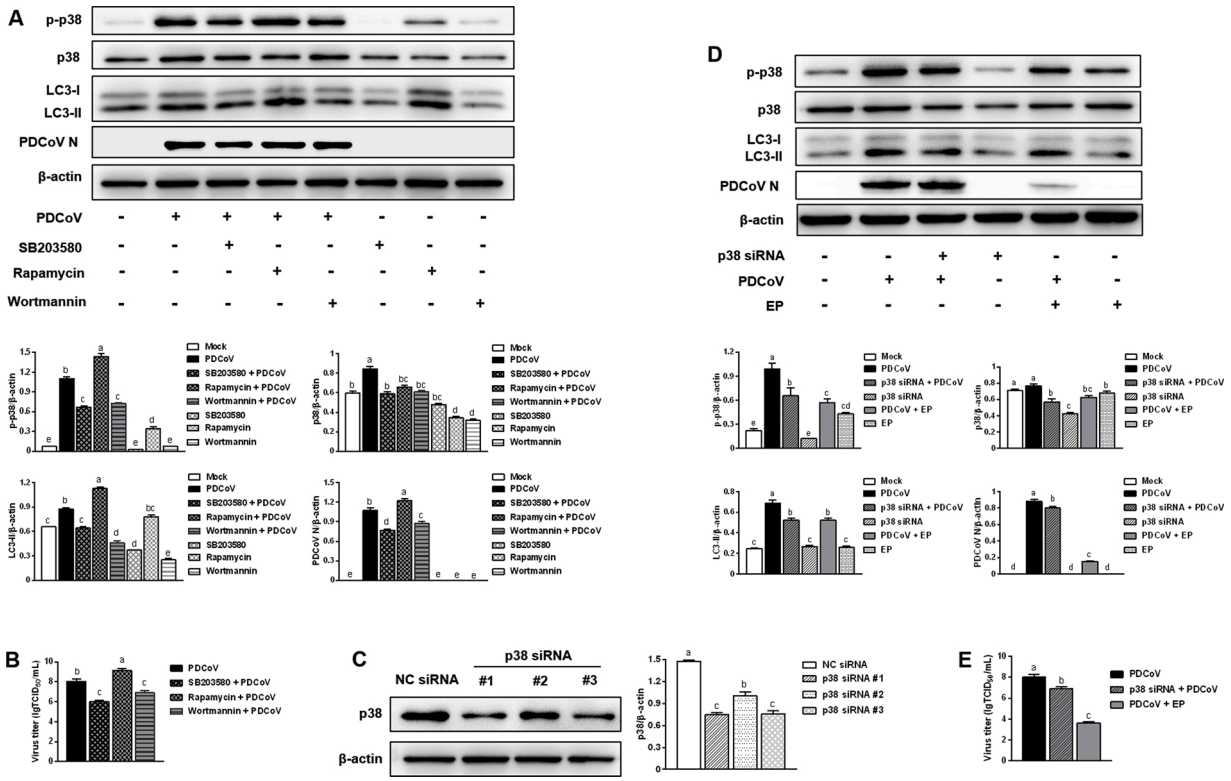

Fig. 5. The p38 signaling pathway participates in the inhibition of EP on PDCoV-induced autophagy. (A) LLC-PK1 cells were pretreated with p38 inhibitor SB203580 (5 μM), rapamycin (62.5 μg/mL) or wortmannin (5 μg/mL) prior to PDCoV infection (MOI = 2). After PDCoV adsorption for 1 h, the cells were further cultured in fresh medium in the absence or presence of SB203580 (5 μM), rapamycin (31.2 μg/mL) or wortmannin (2.5 μg/mL). The expressions of p-p38, p38, LC3-II and PDCoV N were analyzed by western blot at 24 hpi. Results were presented as the ratio of target protein band intensity to β-actin band intensity. (B) The virus titer (lgTCID50/mL) in LLC-PK1 supernatants was calculated by the method of Reed and Muench. (C) The efficiency of p38 siRNA was evaluated by western blot. LLC-PK1 cells were transfected with the indicated siRNA. At 24 h post transfection, the expression of p38 was analyzed by western blot. Results were presented as the ratio of p38 band intensity to β-actin band intensity. (D) LLC-PK1 cells were transfected with p38 siRNA #1 or NC siRNA. At 24 h post transfection, the cells were mock-infected or infected with PDCoV (MOI=2) in the absence or presence EP (150 μM). After PDCoV adsorption for 1 h, the cells were further cultured in fresh medium in the absence or presence EP (150 μM). The expressions of p-p38, p38, LC3-II and PDCoV N were analyzed by western blot at 24 hpi. Results were presented as the ratio of target protein band intensity to β-actin band intensity. Values represent the mean ± SEM for three independent experiments. Mean values without a common superscript (a, b, c, d, e) differ significantly ($P < 0.05$).

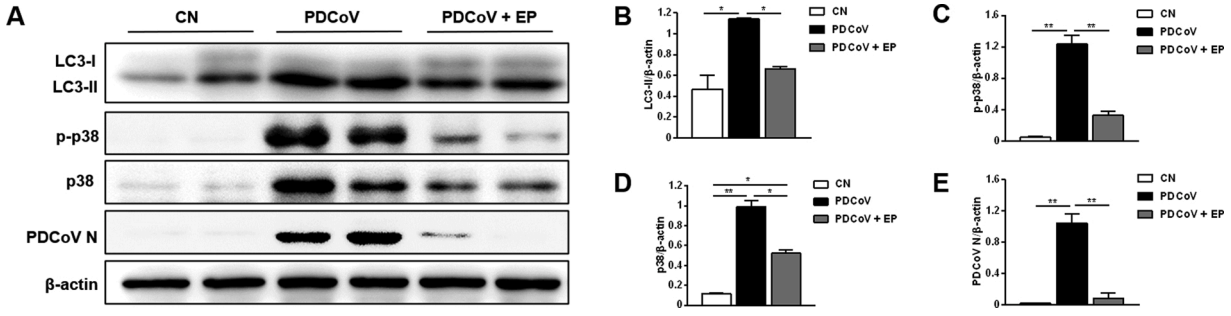

Fig. 6. EP suppressed PDCoV-induced autophagy and p38 activation in the jejunum of piglets.
(A) Western blot analysis of proteins from jejunum tissues probed with the anti-LC3, anti-p-p38, anti-p38 and anti-PDCoV N antibody. (B–E) Results were presented as the ratio of target protein band intensity to β-actin band intensity. Values represent the mean ± SEM for three independent experiments. *$P < 0.05$; **$P < 0.01$.

involves in pathogen infection (Shintani and Klionsky, 2004). On the one hand, host cells utilize autophagy to delivery viruses to the lysosomal compartment for degradation and elimination. On the other hand, many viruses have developed mechanisms to block autophagy or use autophagy for their own benefit. For example, TGEV and PEDV are both swine enteropathogenic coronaviruses. TGEV infection induces autophagy to negatively regulate its replication (Guo et al., 2016), whereas PEDV infection induces autophagy to promote its replication (Lin et al., 2020). Until now, the specific role of autophagy on PDCoV infection has not been reported. In this study, we demonstrated that PDCoV infection induces a complete autophagy and provided the first piece of evidence that PDCoV infection can trigger autophagy to facilitate its replication. We speculated that PDCoV-induced autophagy might provide a membrane platform for its replication or assembly. Besides, autophagy plays multiple roles in innate and adaptive immunity (Levine and Deretic, 2007). It may facilitate virus replication by suppressing innate antiviral immunity. Previous research showed that the ATG12–ATG5 conjugate, a key regulator of the autophagic process, negatively regulated type I IFN

production pathway during vesicular stomatitis virus replication (Jounai et al., 2007). PDCoV-induced autophagy may make for its immune evasion through blocking type I IFN signaling pathway. However, these speculations need further work.

UV-inactivated PDCoV can also induce a degree of autophagy, but it was feebler than the nonirradiated PDCoV. We surmised that PDCoV structural proteins (S, M, E or N) or the attachment process might have the ability to trigger autophagy, and PDCoV replication could enhance the autophagy process. The nonstructural proteins of PDCoV may take part in triggering autophagy. For example, nsp6 and ORF3 of PEDV are two of the key inducers of autophagy (Lin et al., 2020).

So far, there are no adequate control strategies against PDCoV. The development of anti-PDCoV drugs has attracted the attention of an increasing number of researchers (Ke et al., 2021; Zhai et al., 2019). Natural products from Chinese herbs have attracted the attention of pharmacists and have been exploited extensively in the pursuit of new antiviral agents. For example, the application of Traditional Chinese Medicine (TCM) for the treatment or prevention of Severe Acute Respiratory Syndrome Coronavirus (SARS-CoV) and Severe Acute Respiratory Syndrome Coronavirus 2 (SARS-CoV-2) has had an outstanding effect (Yang et al., 2020). Mushrooms have been applied as TCM for centuries, and dried extracts from fruit bodies are a lucrative segment of the market for herbal medicines in western countries (Gründemann et al., 2020). Our previous study revealed that EP from the mushroom *C. volvatus* has efficient anti-PDCoV properties *in vitro* (Duan et al., 2021). In the current study, we found that EP alleviated PDCoV-induced autophagy, contributing to its antiviral effects.

In mammalian cells, the p38 signaling pathway is strongly activated by environmental stresses and inflammatory cytokines. Many viruses, including CoVs, are known to stimulate p38 and to exploit it in order to regulate cellular or viral gene expression or both for the success of virus replication (Lee et al., 2016; Marchant et al., 2010). Thus, p38 can be an effective drug target. At present, we found that knockdown of p38 inhibited PDCoV-induced up-regulation of LC3-II, suggesting that p38 signaling pathway mediates PDCoV-induced autophagy. EP treatment suppressed PDCoV-induced p38 activation, thus alleviating PDCoV-induced autophagy and inhibiting virus replication. Besides, it has been reported that PEDV can induce autophagy *via* the PI3K/Akt/mTOR signaling pathway (Lin et al., 2020). Whether PDCoV also induces autophagy through this pathway remains to be studied.

Autophagy occurs at basal levels in most tissues and contributes to the routine turnover of cytoplasmic components. However, autophagy can be induced by a change of environmental conditions. As far as we know, there is no relevant reports on the effect of PDCoV on autophagy in piglets. Herein, we found that PDCoV infection increased the expressions of LC3-II and phosphorylated p38 in the jejunum, and inferred that PDCoV infection could also induce autophagy through activating p38 signaling pathway *in vivo*. Autophagy can serve to protect cells but may also contribute to cell damage (Shintani and Klionsky, 2004). The induction of autophagy by PDCoV infection may promote its replication in the body and aggravate its damage to the intestine. EP administration reduced p38 activation caused by PDCoV infection, and then attenuated PDCoV-induced autophagy.

In conclusion, this study demonstrates for the first time that PDCoV-induced autophagy enhances virus replication. The p38 signaling pathway mediates the induction of autophagy by PDCoV infection. EP suppresses PDCoV-induced autophagy through p38 signaling pathway to inhibit virus replication *in vitro* and *in vivo*. These results improve the understanding of the pathogenesis of PDCoV infection and provide clues to the development of effective drugs against PDCoV.

Author contributions

Cong Duan and Jiufeng Wang designed the experiments in this study; Cong Duan and Yi Liu performed and analyzed the experiments; Cong Duan, Zhihui Hao and Jiufeng Wang wrote the manuscript.

Declaration of Competing Interest

The authors report no declarations of interest.

Acknowledgement

This study was supported by the National Key R&D Program of China (grant number 2017YFD0502200).

References

Boley, P.A., Alhamo, M.A., Lossie, G., Yadav, K.K., Vasquez-Lee, M., Saif, L.J., Kenney, S. P., 2020. Porcine Deltacoronavirus Infection and Transmission in Poultry, United States[1]. Emerg. Infect. Dis. 26, 55–265. https://doi.org/10.3201/eid2602.190346.

Bonam, S.R., Muller, S., Bayry, J., Klionsky, D.J., 2020. Autophagy as an emerging target for COVID-19: lessons from an old friend, chloroquine. Autophagy 16, 2260–2266. https://doi.org/10.1080/15548627.2020.1779467.

Boya, P., Reggiori, F., Codogno, P., 2013. Emerging regulation and functions of autophagy. Nat. Cell Biol. 15, 713–720. https://doi.org/10.1038/ncb2788.

Dong, N., Fang, L., Yang, H., Liu, H., Du, T., Fang, P., Wang, D., Chen, H., Xiao, S., 2016. Isolation, genomic characterization, and pathogenicity of a Chinese porcine deltacoronavirus strain CHN-HN-2014. Vet. Microbiol. 196, 98–106. https://doi.org/10.1016/j.vetmic.2016.10.022.

Duan, C., Ge, X., Wang, J., Wei, Z., Feng, W.H., Wang, J., 2021. Ergosterol peroxide exhibits antiviral and immunomodulatory abilities against porcine deltacoronavirus (PDCoV) *via* suppression of NF-κB and p38/MAPK signaling pathways *in vitro*. Int. Immunopharmacol. 93, 107317 https://doi.org/10.1016/j.intimp.2020.107317.

Gan, F., Zhou, Y., Qian, G., Huang, D., Hou, L., Liu, D., Chen, X., Wang, T., Jiang, P., Lei, X., Huang, K., 2018. PCV2 infection aggravates ochratoxin A-induced nephrotoxicity *via* autophagy involving p38 signaling pathway *in vivo* and *in vitro*. Environ. Pollut. 238, 656–662. https://doi.org/10.1016/j.envpol.2018.03.032.

Gründemann, C., Reinhardt, J.K., Lindequist, U., 2020. European medicinal mushrooms: do they have potential for modern medicine? - An update. Phytomedicine 66, 153131. https://doi.org/10.1016/j.phymed.2019.153131.

Guo, L., Yu, H., Gu, W., Luo, X., Li, R., Zhang, J., Xu, Y., Yang, L., Shen, N., Feng, L., Wang, Y., 2016. Autophagy negatively regulates transmissible gastroenteritis virus replication. Sci. Rep. 6, 23864. https://doi.org/10.1038/srep23864.

Hou, L.J., Xie, M.Y., Ye, W.C., Zhao, G.J., 2020. Doxycycline ameliorates autophagy by inhibiting p38 MAPK in cardiac myocytes. Int. J. Cardiol. S0167-5273, 34286–34288. https://doi.org/10.1016/j.ijcard.2020.12.038.

Hua, Q., Sun, J., Shen, L., 1991. Biological characteristics of *Cryptoporus volvatus* (peck) Hubb., a medicinal fungus. Zhongguo Zhong Yao Za Zhi 16 (719-722), 761.

Jang, G., Lee, K.K., Kim, S.H., Lee, C., 2017. Prevalence, complete genome sequencing and phylogenetic analysis of porcine deltacoronavirus in South Korea, 2014-2016. Transbound. Emerg. Dis. 64, 1364–1370. https://doi.org/10.1111/tbed.12690.

Jounai, N., Takeshita, F., Kobiyama, K., Sawano, A., Miyawaki, A., Xin, K.Q., Ishii, K.J., Kawai, T., Akira, S., Suzuki, K., Okuda, K., 2007. The Atg5 Atg12 conjugate associates with innate antiviral immune responses. Proc. Natl. Acad. Sci. U. S. A. 104, 14050–14055. https://doi.org/10.1073/pnas.0704014104.

Jung, K., Hu, H., Saif, L.J., 2017. Calves are susceptible to infection with the newly emerged porcine deltacoronavirus, but not with the swine enteric alphacoronavirus, porcine epidemic diarrhea virus. Arch. Virol. 162, 2357–2362. https://doi.org/10.1007/s00705-017-3351-z.

Ke, W., Wu, X., Fang, P., Zhou, Y., Fang, L., Xiao, S., 2021. Cholesterol 25-hydroxylase suppresses porcine deltacoronavirus infection by inhibiting viral entry. Virus Res. 295, 198306 https://doi.org/10.1016/j.virusres.2021.198306.

Lee, C., Kim, Y., Jeon, J.H., 2016. JNK and p38 mitogen-activated protein kinase pathways contribute to porcine epidemic diarrhea virus infection. Virus Res. 222, 1–12. https://doi.org/10.1016/j.virusres.2016.05.018.

Levine, B., Deretic, V., 2007. Unveiling the roles of autophagy in innate and adaptive immunity. Nat. Rev. Immunol. 7, 767–777. https://doi.org/10.1038/nri2161.

Levine, B., Kroemer, G., 2008. Autophagy in the pathogenesis of disease. Cell 132, 27–42. https://doi.org/10.1016/j.cell.2007.12.018.

Lin, H., Li, B., Liu, M., Zhou, H., He, K., Fan, H., 2020. Nonstructural protein 6 of porcine epidemic diarrhea virus induces autophagy to promote viral replication *via* the PI3K/Akt/mTOR axis. Vet. Microbiol. 244, 108684. https://10.1016/j.vetmic.2020.108684.

Ma, Z., Zhang, W., Wang, L., Zhu, M., Wang, H., Feng, W.H., Ng, T.B., 2013. A novel compound from the mushroom *Cryptoporus volvatus* inhibits porcine reproductive and respiratory syndrome virus (PRRSV) *in vitro*. PLoS One 8, e79333. https://doi.org/10.1371/journal.pone.0079333.

Ma, Y., Zhang, Y., Liang, X., Lou, F., Oglesbee, M., Krakowka, S., Li, J., 2015. Origin, evolution, and virulence of porcine deltacoronaviruses in the United States. mBio 6, e00064. https://doi.org/10.1128/mBio.00064-15.

Marchant, D., Singhera, G.K., Utokaparch, S., Hackett, T.L., Boyd, J.H., Luo, Z., Si, X., Dorscheid, D.R., McManus, B.M., Hegele, R.G., 2010. Toll-like receptor 4-mediated activation of p38 mitogen-activated protein kinase is a determinant of respiratory virus entry and tropism. J. Virol. 84, 11359–11373. https://doi.org/10.1128/JVI.00804-10.

Mizushima, N., Yoshimori, T., Levine, B., 2010. Methods in mammalian autophagy research. Cell 140, 313–326. https://doi.org/10.1016/j.cell.2010.01.028.

Pei, J., Zhao, M., Ye, Z., Gou, H., Wang, J., Lin, Y., Dong, X., Liu, W., Luo, Y., Liao, M., Chen, J., 2014. Autophagy enhances the replication of classical swine fever virus *in vitro*. Autophagy 10, 93–110. https://doi.org/10.4161/auto.26843.

Qin, P., Du, E.Z., Luo, W.T., Yang, Y.L., Zhang, Y.Q., Wang, B., Huang, Y.W., 2019. Characteristics of the life cycle of porcine deltacoronavirus (PDCoV) *in vitro*: replication kinetics, cellular ultrastructure and virion morphology, and evidence of inducing autophagy. Viruses 11, 455. https://doi.org/10.3390/v11050455.

Shintani, T., Klionsky, D.J., 2004. Autophagy in health and disease: a double-edged sword. Science 306, 990–995. https://doi.org/10.1126/science.1099993.

Sun, M.X., Huang, L., Wang, R., Yu, Y.L., Li, C., Li, P.P., Hu, X.C., Hao, H.P., Ishag, H.A., Mao, X., 2012. Porcine reproductive and respiratory syndrome virus induces autophagy to promote virus replication. Autophagy 8, 1434–1447. https://doi.org/10.4161/auto.21159.

Suzuki, T., Shibahara, T., Imai, N., Yamamoto, T., Ohashi, S., 2018. Genetic characterization and pathogenicity of Japanese porcine deltacoronavirus. Infect. Genet. Evol. 61, 176–182. https://doi.org/10.1016/j.meegid.2018.03.030.

Valero-Muñoz, M., Wilson, R.M., Bretón-Romero, R., Croteau, D., 2020. Doxycycline decreases amyloidogenic light chain-induced autophagy in isolated primary cardiac myocytes. Int. J. Cardiol. 321, 133–136. https://doi.org/10.1016/j.ijcard.2020.07.016.

Wang, L., Byrum, B., Zhang, Y., 2014. Detection and genetic characterization of deltacoronavirus in pigs, Ohio, USA, 2014. Emerg. Infect. Dis. 20, 1227–1230. https://doi.org/10.3201/eid2007.140296.

Woo, P.C.Y., Lau, S.K.P., Lam, C.S.F., Lau, C.C.Y., Tsang, A.K.L., Lau, J.H.N., Bai, R., Teng, J.L.L., Tsang, C.C.C., Wang, M., Zheng, B.J., Chan, K.H., 2012. Discovery of seven novel Mammalian and avian coronaviruses in the genus deltacoronavirus supports bat coronaviruses as the gene source of alphacoronavirus and betacoronavirus and avian coronaviruses as the gene source of gammacoronavirus and deltacoronavirus. J. Virol. 86, 3995–4008. https://doi.org/10.1128/JVI.06540-11.

Xie, Q.M., Deng, J.F., Deng, Y.M., Shao, C.S., Zhang, H., Ke, C.K., 2006. Effects of cryptoporus polysaccharide on rat allergic rhinitis associated with inhibiting eotaxin mRNA expression. J. Ethnopharmacol. 107, 424–430. https://doi.org/10.1016/j.jep.2006.03.040.

Yang, Y., Islam, M.S., Wang, J., Li, Y., Chen, X., 2020. Traditional Chinese Medicine in the treatment of patients infected with 2019-new Coronavirus (SARS-CoV-2): a review and perspective. Int. J. Biol. Sci. 16, 1708–1717. https://doi.org/10.7150/ijbs.45538.

Zhai, X., Wang, S., Zhu, M., He, W., Pan, Z., Su, S., 2019. Antiviral effect of lithium chloride and diammonium glycyrrhizinate on porcine deltacoronavirus *in vitro*. Pathogens 8, 144. https://doi.org/10.3390/pathogens8030144.

Zhu, J.P., Wu, K., Li, J.Y., Guan, Y., Sun, Y.H., Ma, W.J., Xie, Q.M., 2016. *Cryptoporus volvatus* polysaccharides attenuate LPS-induced expression of pro-inflammatory factors *via* the TLR2 signaling pathway in human alveolar epithelial cells. Pharm. Biol. 4, 347–353. https://doi.org/10.3109/13880209.2015.1042981.